Electron–phonon interactions in the $w = 0$ pairing scenario

2004 J. Phys.: Condens. Matter 16 4845

(http://iopscience.iop.org/0953-8984/16/28/007)

INSTITUTE OF PHYSICS PUBLISHING JOURNAL OF PHYSICS: CONDENSED MATTER

J. Phys.: Condens. Matter **16** (2004) 4845–4866 PII: S0953-8984(04)77288-4

Electron–phonon interactions in the $W = 0$ pairing scenario

Enrico Perfetto and Michele Cini

Dipartimento di Fisica, Universita' di Roma Tor Vergata, Via della Ricerca Scientifica, 1-00133 Roma, Italy
and
INFN, Laboratori Nazionali di Frascati, CP 13, 00044 Frascati, Italy

Received 3 March 2004
Published 2 July 2004
Online at stacks.iop.org/JPhysCM/16/4845
doi:10.1088/0953-8984/16/28/007

Abstract

We investigate the interplay of phonons and correlations in superconducting pairing by introducing a model Hamiltonian with on-site repulsion and couplings to several vibration branches having the Cu–O plane of the cuprates as a paradigm. We express the electron–phonon (EP) coupling through two force constants for O–Cu and O–O bond stretchings. Without phonons, this reduces to the Hubbard model, and allows purely electronic $W = 0$ pairing. A $W = 0$ pair is a two-body singlet eigenstate of the Hubbard Hamiltonian, with no double occupancy, which gets bound via interactions with background particles. Indeed, this mechanism produces a Kohn–Luttinger-like pairing from the Hubbard repulsion, provided that its symmetry is not severely distorted. From the many-body theory, a canonical transformation extracts the effective two-body problem, which lends itself to numerical analysis in case studies. As a test, we use as a prototype system the CuO_4 cluster. We show analytically that at weak EP coupling the additive contributions of the half-breathing modes reinforce the electronic pairing. At intermediate and strong EP coupling and $U \sim t$, the model behaves in a complex and intriguing way.

(Some figures in this article are in colour only in the electronic version)

1. Introduction

While the Fröhlich mechanism of conventional superconductivity is driven by phonon exchange, the pairing mechanism in highly correlated narrow band systems could have a predominantly electronic origin [1] and the Cu–O plane of cuprates is the most frequently discussed example. Although this remains a very controversial issue, most authors probably accept at least the conceptual importance of a lattice counterpart of the Kohn–Luttinger idea [2] that attractive interactions result from mere repulsion. The renormalization group approach [3]

to the Hubbard model shows that such a superconducting instability in the $d_{x^2-y^2}$ channel is dominant near half-filling, confirming the results obtained with the FLEX approximation [4]. One definition of pairing is $\tilde{\Delta} < 0$, where

$$\tilde{\Delta}(N+2) = E(N+2) + E(N) - 2E(N+1), \tag{1}$$

and $E(N)$ is the ground state energy of the system with N fermions; this criterion is suitable for finite cluster calculations by exact diagonalization methods. $\tilde{\Delta} < 0$ was indeed observed in particular Hubbard clusters [5, 6], but in many other examples with on-site repulsion on every site a large $\tilde{\Delta} > 0$ was found [7, 8]. The $W = 0$ theory [9–11] gives a systematic method for producing and analysing examples of singlet pairing by repulsive interactions; it also allows validating $|\tilde{\Delta}|$ as the pairing binding energy. In this framework the non-Abelian symmetry group of the underlying graph and the resulting degeneracy are crucial for the pairing mechanism. The fillings and the symmetry channels where the $W = 0$ pairing can occur are determined in full generality by the $W = 0$ theorem [12]; these symmetries achieve the same result as high angular momentum and parallel spins in the Kohn–Luttinger [2] continuum approach.

Anyway, a purely electronic theory misses practically and conceptually important features of this complicated problem. First, many high T_C compounds exhibit a quite noticeable doping-dependent isotope effect [13], suggesting that electron–phonon (EP) interactions are important and should be included in the theory. In addition, there is experimental evidence [14] that the half-breathing Cu–O bond stretching mode at $k = (\pi, 0), (0, \pi)$ is significantly coupled with the doped holes in the superconducting regime and its contribution may be relevant for the $d_{x^2-y^2}$ pairing [15–17]. A radical, yet serious criticism of all electronic mechanisms was put forward by Mazumdar and co-workers [18]. They suggested that any pairing in Hubbard clusters has doubtful physical interpretation due to the neglect of the lattice degrees of freedom and the Jahn–Teller (JT) effect. They argued that JT distortions might well cause a larger energy gain of the system with $N + 1$ particles, and that could reverse the sign of $\tilde{\Delta}$ obtained at fixed nuclei; in this case the pairing would be just an artefact of the Hubbard model. This even led the authors to the conjecture that any $\tilde{\Delta} < 0$ due to an electronic mechanism is just a finite size effect, which vanishes for large systems like the JT effect does. Below, we shall show that the Mazumdar *et al* argument [18], based on a static Jahn–Teller approximation, can break down in a peculiar and nontrivial way when more flexible wavefunctions are allowed; thus, phonon pairing and $W = 0$ pairing can be compatible, depending on the symmetries of both the pair and vibration and on frequencies.

The Hubbard–Holstein model, where electrons are coupled to a local Einstein phonon, provides a simple way to include both strong electronic correlations and EP interactions. Much is known about the possibility of a superconducting phase in this model. Pao and Schuttler [19] applied the numerical renormalization group techniques within the FLEX approximation and found that in the square geometry s-wave pairing is enhanced by phonons, while $d_{x^2-y^2}$ pairing is suppressed. In the strong EP regime a Lang–Firsov [20] transformation maps the Hubbard–Holstein model in an effective Hamiltonian for hopping polarons with a screened on-site interaction $\tilde{U} = U - \frac{g^2}{\omega}$, where U is the Hubbard repulsion, ω is the phonon frequency, and g is the EP coupling constant. If overscreening is attained, $\tilde{U} < 0$ becomes an effective attraction and one gets bipolaronic bound states [21, 22]; however, it is still unclear whether they can exist as itinerant band states [23, 24]. Petrov and Egami [25] found $\tilde{\Delta} < 0$ in a doped eight-site Hubbard–Holstein ring at strong enough EP coupling, while otherwise the normal repulsion prevails. This situation is unavoidable in the one-dimensional repulsive Hubbard model, where no superconducting pairing exists.

In this paper we take the view that one of the sound experimental facts about the CuO plane in all cuprates is that the geometry permits $W = 0$ pairs which avoid completely the strong hole–hole repulsion. It is therefore highly plausible that such pairs are important ingredients of the theory, provided that there is a way out of the Mazumdar *et al* [18] argument. Anyway, it is not obvious that the phonons will reinforce the attraction while preserving the symmetry. More generally, some vibrations could be pairing and others pair breaking. When lattice effects are introduced in the $W = 0$ scenario, the situation is very different from the Petrov and Egami [25] model, when, as in the conventional (Fröhlich) mechanism, phonons overscreen the electron repulsion; what happens if electronic screening already leads to pairing?

To address these problems we use an extension of the Hubbard model in which bond stretchings dictate the couplings to the normal modes of the C_{4v}-symmetric configuration. This is physically more detailed than the Hubbard–Holstein model, and is not restricted to on-site EP couplings that would be impaired by a strong Hubbard repulsion.

The plan of the paper is the following. After introducing the model Hamiltonian in the next section, we devote section 3 to a detailed derivation of the effective interactions between holes in the $W = 0$ pair, which is obtained by extending a previous Hubbard model treatment. Our canonical transformation approach is quite general for weak EP coupling and corresponds to the inclusion of all diagrams involving one-phonon and electron–hole pair exchange due to correlations. We specialize in section 4 to the prototype CuO_4 cluster, describing electronic states and vibration modes. The effective interaction is calculated explicitly in section 5. Next, we develop a theory based on the Jahn–Teller operator in section 6; in this way we want to test the reliability of that approximation in modelling the behaviour of $W = 0$ pairs in the presence of Jahn–Teller-active modes. The numerical results of the full theory are then exposed and discussed in section 7; the exact data for realistic vibration frequencies disagree from those of section 6 but are in accord with the canonical transformation approach of section 5. The agreement is excellent at weak coupling, but the analytical approach is qualitatively validated also at intermediate coupling. Finally section 8 is devoted to the conclusions.

2. Model

We start from the Hubbard model with on-site interaction U and expand the hopping integrals $t_{i,j}(\mathbf{r}_i, \mathbf{r}_j)$ in powers of the displacements $\boldsymbol{\rho}_i$ around a C_{4v}-symmetric equilibrium configuration:

$$t_{i,j}(\mathbf{r}_i, \mathbf{r}_j) \simeq t^0_{i,j}(\mathbf{r}_i, \mathbf{r}_j) + \sum_\alpha \left[\frac{\partial t_{ij}(\mathbf{r}_i, \mathbf{r}_j)}{\partial r^\alpha_i}\right]_0 \rho^\alpha_i + \sum_\alpha \left[\frac{\partial t_{ij}(\mathbf{r}_i, \mathbf{r}_j)}{\partial r^\alpha_j}\right]_0 \rho^\alpha_j, \quad (2)$$

where $\alpha = x, y$. Below, we write down the ρ^α_i in terms of the normal modes $q_{\eta\nu}$: $\rho^\alpha_i = \sum_{\eta\nu} S^\alpha_{\eta\nu}(i) q_{\eta\nu}$, where η is the label of an irreducible representation (irrep) of the symmetry group of the undistorted system and ν is a phonon branch.

Thus, treating the Cu atoms as fixed, for simplicity, one can justify an electron–lattice Hamiltonian:

$$H_{\text{el-latt}} = H_0 + V_{\text{tot}}. \quad (3)$$

Here $H_0 = H^{\text{n}}_0 + H^{\text{e}}_0$ is given by

$$H_0 = \sum_\eta \hbar\omega_{\eta,\nu} b^\dagger_{\eta,\nu} b_{\eta,\nu} + \sum_{i,j\sigma} t^0_{i,j}(\mathbf{r}_i, \mathbf{r}_j)(c^\dagger_{i\sigma} c_{j\sigma} + \text{h.c.}), \quad (4)$$

where $\omega_{\eta,\nu}$ are the frequencies of the normal modes with creation operator $b^\dagger_{\eta,\nu}$, while $c^\dagger_{i\sigma}$ creates a fermion of spin σ in site i. Moreover, let M denote the O mass, $\xi_{\eta,\nu} = \lambda_{\eta\nu}\sqrt{\frac{\hbar}{2M\omega_{\eta,\nu}}}$,

with $\lambda_{\eta\nu}$ numbers of order unity that modulate the EP coupling strength. Then, $V_{\rm tot} = V + W$ reads

$$V_{\rm tot} = \sum_{\eta,\nu} \xi_{\eta,\nu}(b^{\dagger}_{\eta,\nu} + b_{\eta,\nu}) H_{\eta,\nu} + U \sum_{i} n_{i\uparrow} n_{i\downarrow}; \tag{5}$$

the $H_{\eta,\nu}$ operators are given by

$$H_{\eta,\nu} = \sum_{i,j} \sum_{\alpha,\sigma} \left\{ S^{\alpha}_{\eta\nu}(i) \left[\frac{\partial t_{ij}(\mathbf{r}_i, \mathbf{r}_j)}{\partial r^{\alpha}_i} \right]_0 + S^{\alpha}_{\eta\nu}(j) \left[\frac{\partial t_{ij}(\mathbf{r}_i, \mathbf{r}_j)}{\partial r^{\alpha}_j} \right]_0 \right\} (c^{\dagger}_{i,\sigma} c_{j,\sigma} + \text{h.c.}). \tag{6}$$

In previous work we have shown that the pure Hubbard model $H_{\rm H} = H^{\rm e}_0 + W$ defined on the Cu–O plane and on the simple square also admits two-body singlet eigenstates with no double occupancy on lattice sites. We referred to them as $W = 0$ pairs. $W = 0$ pairs are therefore eigenstates of the kinetic energy operator $H^{\rm e}_0$ and of the Hubbard repulsion W with vanishing eigenvalue of the latter. The particles forming a $W = 0$ pair have no direct interaction and are the main candidates for achieving bound states in purely repulsive Hubbard models [26–28]. In order to study whether the $W = 0$ can actually form bound states in the many-body interacting problem, we developed a canonical transformation of the Hubbard Hamiltonian [26], which enables us to extract the effective interaction between the particles forming the pairs. Pairing was found in small symmetric clusters and large systems as well.

In the next section we wish to derive an effective interaction between the particles in the pair suitable for $H_{\rm el-latt}$, by generalizing the canonical transformation approach of [26].

3. Canonical transformation

In this section we assume that the system has periodic boundary conditions with particle number N; we denote the phonon vacuum by $|0\rangle\rangle$ and the non-interacting Fermi sphere by $|\Phi_0(N)\rangle$. The creation operator of a $W = 0$ pair is obtained [12] by applying an appropriate projection operator to $c^{\dagger}_{k\uparrow} c^{\dagger}_{k'\downarrow}$, where the labels denote Bloch states. If we add a $W = 0$ pair to $|\Phi_0(N)\rangle \otimes |0\rangle\rangle$, the two extra particles, by definition, cannot interact directly (in first order). Hence their effective interaction comes out from virtual electron–hole (e–h) excitation and/or phonon exchange and in principle can be attractive. To expand the interacting $(N+2)$-fermion ground state $|\Psi_0(N+2)\rangle$, we build a complete set of configurations in the subspace with vanishing z spin component, considering the vacuum state $|\Phi_0(N)\rangle \otimes |0\rangle\rangle$ and the set of excitations over it.

We start by creating $W = 0$ pairs of fermions over $|\Phi_0(N)\rangle \otimes |0\rangle\rangle$; we denote by $|m\rangle \otimes |0\rangle\rangle$ these states. At weak coupling, we may truncate the Hilbert space to the simplest excitations, i.e., to states involving one e–h pair or one phonon created over the $|m\rangle \otimes |0\rangle\rangle$ states. We define the $|m\rangle \otimes |q\rangle\rangle$ states, obtained by creating a phonon denoted by $q = (\eta, \nu)$ over the $|m\rangle \otimes |0\rangle\rangle$ states. Finally, we introduce the $|\alpha\rangle \otimes |0\rangle\rangle$ states, obtained from the $|m\rangle \otimes |0\rangle\rangle$ states by creating one electron–hole (e–h) pair.

The approximation can be systematically improved by including two or more electron–hole pairs and excitations in the truncated Hilbert space, at the cost of heavier computation.

We now expand the interacting ground state in the truncated Hilbert space:

$$|\Psi_0(N+2)\rangle = \sum_{m} a_m |m\rangle \otimes |0\rangle\rangle + \sum_{m,q} a_{m,q} |m\rangle \otimes |q\rangle\rangle + \sum_{\alpha} a_{\alpha} |\alpha\rangle \otimes |0\rangle\rangle \tag{7}$$

and set up the Schrödinger equation

$$H_{\rm el-latt} |\Psi_0(N+2)\rangle = E |\Psi_0(N+2)\rangle. \tag{8}$$

We now consider the effects of the operators H_0 and $V_{\rm tot}$ on the terms of $|\Psi_0(N+2)\rangle$. Choosing the $|m\rangle \otimes |0,q\rangle\rangle$, $|\alpha\rangle \otimes |0\rangle\rangle$ states to be eigenstates of the noninteracting term H_0 we have, understanding $\hbar$,

$$H_0|m\rangle \otimes |0\rangle\rangle = E_m|m\rangle \otimes |0\rangle\rangle, \tag{9}$$

$$H_0|m\rangle \otimes |q\rangle\rangle = (E_m + \omega_q)|m\rangle \otimes |q\rangle\rangle, \tag{10}$$

$$H_0|\alpha\rangle \otimes |0\rangle\rangle = E_\alpha|\alpha\rangle \otimes |0\rangle\rangle. \tag{11}$$

Let us consider the action of V and W on the same states, taking into account that V creates or annihilates up to one phonon and one e–h pair, and W is diagonal in the phonon states and can create or destroy up to two e–h pairs:

$$(V+W)|m\rangle \otimes |0\rangle\rangle = \sum_{m',q} V^q_{m,m'}|m'\rangle \otimes |q\rangle\rangle + \sum_{m'} W_{m,m'}|m'\rangle \otimes |0\rangle\rangle + \sum_{\alpha} W_{m,\alpha}|\alpha\rangle \otimes |0\rangle\rangle, \tag{12}$$

$$(V+W)|m\rangle \otimes |q\rangle\rangle = \sum_{m'} V^q_{m,m'}|m'\rangle \otimes |0\rangle\rangle + \sum_{\alpha} V^q_{m,\alpha}|\alpha\rangle \otimes |0\rangle\rangle + \sum_{m'} W_{m,m'}|m'\rangle \otimes |q\rangle\rangle, \tag{13}$$

$$(V+W)|\alpha\rangle \otimes |0\rangle\rangle = \sum_{m',q} V^q_{\alpha,m'}|m'\rangle \otimes |q\rangle\rangle + \sum_{\alpha'} W_{\alpha,\alpha'}|\alpha'\rangle \otimes |0\rangle\rangle + \sum_{m} W_{\alpha,m}|m\rangle \otimes |0\rangle\rangle. \tag{14}$$

The Schrödinger equation yields three coupled equations for the coefficients a:

$$(E_m - E)a_m + \sum_{m'} a_{m'}W_{m,m'} + \sum_{m',q} a_{m',q}V^q_{m,m'} + \sum_{\alpha} a_\alpha W_{m,\alpha} = 0; \tag{15}$$

$$(E_m + \omega_q - E)a_{m,q} + \sum_{m'} a_{m',q}W_{m,m'} + \sum_{m'} a_{m'}V^q_{m,m'} + \sum_{\alpha} a_\alpha V^q_{m,\alpha} = 0; \tag{16}$$

$$(E_\alpha - E)a_\alpha + \sum_{\alpha'} a_{\alpha'}W_{\alpha,\alpha'} + \sum_{m} a_m W_{\alpha,m} + \sum_{m,q} a_{m,q}V^q_{\alpha,m} = 0. \tag{17}$$

We define renormalized eigenenergies E'_α by taking a linear combination of the α states in such a way that

$$(H_0 + W)_{\alpha,\alpha'} = \delta_{\alpha\alpha'}E'_\alpha. \tag{18}$$

Equation (17) can be solved for the a_α coefficients:

$$a_\alpha = \frac{1}{E'_\alpha - E}\left(\sum_m a_m W_{\alpha,m} + \sum_{m,q} a_{m,q}V^q_{\alpha,m}\right). \tag{19}$$

Substituting a_α in equation (16) one gets

$$(E_m + \omega_q - E)a_{m,q} + \sum_{m'} a_{m',q}W_{m,m'} + \sum_{m'} a_{m'}V^q_{m,m'} + \sum_{m',q'} a_{m',q'}\left(\sum_\alpha \frac{V^q_{m,\alpha}V^{q'}_{\alpha,m'}}{E'_\alpha - E}\right) + \sum_{m'} a_{m'}\left(\sum_\alpha \frac{V^q_{m,\alpha}W_{\alpha,m'}}{E'_\alpha - E}\right) = 0. \tag{20}$$

Here, two important simplifications allow us to proceed. First, as in [10], equation (49), one can show that

$$W_{m,m'} = W^{(\rm d)}_{m,m'} + \delta_{m,m'}W_{\rm F}; \tag{21}$$

$W^{(\mathrm{d})}_{m,m'}$ is the direct interaction among the particles forming the pair and W_{F} comes from the average over the occupied states on the Fermi sphere and is an m-independent constant; since $W^{(\mathrm{d})}_{m,m'}$ vanishes for the $W = 0$ property, it holds that

$$\sum_{m'} a_{m',q} W_{m,m'} = a_{m,q} W_{\mathrm{F}}. \tag{22}$$

Moreover,

$$\sum_{m',q'} a_{m',q'} \left(\sum_{\alpha} \frac{V^{q}_{m,\alpha} V^{q'}_{\alpha,m'}}{E'_{\alpha} - E} \right) = a_{m,q} \left(\sum_{\alpha} \frac{|V^{q}_{m,\alpha}|^2}{E'_{\alpha} - E} \right). \tag{23}$$

Indeed, V is a one-body operator for the fermions; so the electron–hole pair in the α state must be created by one V factor and annihilated by the other; in this way, the $W = 0$ pair is not touched. With these simplifications, the contributions in equations (22) and (23) can be taken over to the lhs of equation (20), where they just renormalize the eigenenergies of the $|m\rangle \otimes |q\rangle\rangle$ states. Thus, $E_m + \omega_q \to E'_m + \omega_q$, and equation (20) can easily solved for the $a_{m,q}$, as we did for the a_{α} in equation (19):

$$a_{m,q} = \frac{1}{E'_m + \omega_q - E} \sum_{m'} a_{m'} \left(V^{q}_{m,m'} + \sum_{\alpha} \frac{V^{q}_{m,\alpha} W_{\alpha,m'}}{E'_{\alpha} - E} \right). \tag{24}$$

Finally, substituting equations (19), (24) into (15), we can write the Schrödinger equation in terms of only the $|m\rangle$ states, with the excitation-mediated interactions and with renormalized quantities:

$$\begin{aligned} 0 = (E_m - E) a_m + a_m W_{\mathrm{F}} &+ \sum_{m',m'',q} a_{m'} \frac{V^{q}_{m,m''} V^{q}_{m'',m'}}{E'_{m''} + \omega_q - E} + \sum_{m',\alpha} a_{m'} \frac{W_{m,\alpha} W_{\alpha,m'}}{E'_{\alpha} - E} \\ &+ 2 \sum_{m',m'',q,\alpha} a_{m'} \frac{V^{q}_{m,m''} V^{q}_{m'',\alpha} W_{\alpha,m'}}{(E'_{m''} + \omega_q - E)(E'_{\alpha} - E)} \\ &+ \sum_{m',m'',q,\alpha,\alpha'} a_{m'} \frac{W_{m,\alpha} V^{q}_{\alpha,m''} V^{q}_{m'',\alpha'} W_{\alpha',m'}}{(E'_{m''} + \omega_q - E)(E'_{\alpha} - E)(E'_{\alpha'} - E)}. \end{aligned} \tag{25}$$

Here, the last two terms are of higher order and must be dropped; E is the ground state of the system with $N + 2$ fermions; however, equation (25) is of the form of a Schrödinger equation with eigenvalue E for the added pair. We interpret the a_m as the coefficients in the expansion over the $W = 0$ pairs of the wavefunction of the dressed pair, $|\varphi\rangle \equiv \sum_m a_m |m\rangle \otimes |0\rangle\rangle$. This obeys the Cooper-like equation

$$H_{\mathrm{pair}} |\varphi\rangle = E |\varphi\rangle \tag{26}$$

with the same E as in equation (8), but with an effective two-body Hamiltonian:

$$H_{\mathrm{pair}} \equiv H_0 + W_{\mathrm{F}} + S[E]. \tag{27}$$

Here S is the E-dependent effective scattering operator

$$S[E]_{m,m'} = \sum_{\alpha} \frac{W_{m,\alpha} W_{\alpha,m'}}{E'_{\alpha} - E} + \sum_{m'',q} \frac{V^{q}_{m,m''} V^{q}_{m'',m'}}{E'_{m''} + \omega_q - E}, \tag{28}$$

and therefore equation (26) must be solved self-consistently. Let us examine in detail the structure of the $S[E]$ contribution. The matrix elements $S_{m,m'}$ may be written as

$$S_{m,m'} = (W_{\mathrm{eff}})_{m,m'} + F_m \delta_{m,m'}, \tag{29}$$

where $W_{\rm eff}$ is the true effective interaction between the electrons in the m states, while the other term represents the forward scattering amplitude F.

The first-order self-energy $W_{\rm F}\delta_{m,m'}$ and the forward scattering term $F_m\delta_{m,m'}$ are diagonal in the indices m and m', and therefore they renormalize the non-interacting energy E_m of the m states:

$$E_m \to E_m^{(\rm R)} = E_m + W_{\rm F} + F_m. \tag{30}$$

If the effective interaction $W_{\rm eff}$ is attractive and produces bound, localized states, the spectrum of the Schrödinger equation with the Hamiltonian in equation (27) contains discrete states below the unpaired states. In an extended system, we have bound states below the threshold of the *continuum*. The threshold may be defined (in clusters and in extended systems) by

$$E_{\rm T}^{(\rm R)} \equiv \min_{\{m\}}[E_m^{(\rm R)}(E)], \tag{31}$$

which, according to equation (30), takes into account all the pairwise interactions except those between the particles in the pair. Note that this is an extensive quantity, i.e. an $(N+2)$-particle energy. The ground state energy E may be conveniently written as

$$E = E_{\rm T}^{(\rm R)} + \Delta; \tag{32}$$

$\Delta < 0$ indicates a Cooper-like instability of the normal Fermi liquid and its magnitude represents the binding energy of the pair.

Below, we solve equation (26) explicitly for the CuO_4 cluster with open boundary conditions, where the above theory is readily applied.

4. Prototype cluster

As an illustrative application of the above pairing scheme, in this preliminary work we focus on CuO_4, the smallest cluster yielding $W = 0$ pairing in the Hubbard model. This requires four holes (total number, not referred to half-filling); such a doping is somewhat unrealistic, but larger C_{4v}-symmetric clusters and the full CuO_2 plane also show $W = 0$ pairing in the doping regime relevant for cuprates [9, 26]. Remarkably, in the pure Hubbard model, one can verify that $\Delta = \tilde{\Delta}(4)$ at least at weak coupling [9], which demonstrates that $\tilde{\Delta}$ has the physical meaning of an effective interaction. CuO_4 represents a good test of the interplay between electronic and phononic pairing mechanisms since we can compare exact diagonalization results with the analytic approximations of the canonical transformation. A further merit of this model is that it demonstrates dramatically the decisive role of symmetry in the electronic pairing mechanism: any serious distortion of the square symmetry restores the normal $\tilde{\Delta} > 0$ situation [9]. Since vibrations cause distortions it is not evident *a priori* that they tend to help pairing; in particular, we may expect Jahn–Teller distortions to prevent $W = 0$ pairing altogether. On the other hand, the Fröhlich mechanism of conventional superconductivity is based on phonon exchange. This suggests that the role of EP coupling is complex.

CuO_4 allows only coupling to phonons at the centre or at the edge of the Brillouin zone; however, phonons near the edge are precisely those most involved [14, 15]. Even in this small system the virtually exact diagonalizations are already hard and the next C_{4v}-symmetric example, the Cu_5O_4 cluster [27], is much more demanding because of the number of vibrations and the size of the electronic Hilbert space.

Starting with the C_{4v}-symmetric arrangement, any displacement of the oxygens in the plane can be analysed in irreps, A_1, A_2, B_1, B_2, E_1, E_2; see figure 1.

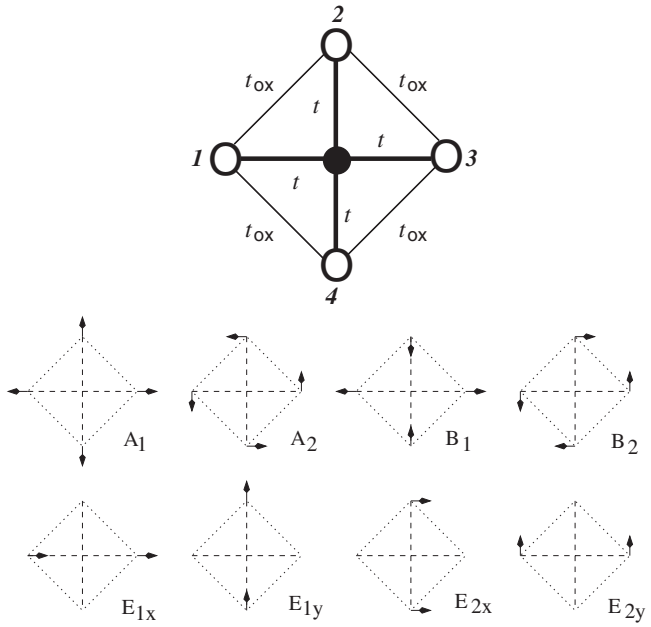

Figure 1. A pictorial representation of the ionic displacements in the eight normal modes of the CuO_4 cluster, labelled according to the irreps of the C_{4v} Group.

We suppose that the hopping integrals depend only on the bond lengths[1]. Hence, the EP coupling is expressed through just two parameters g and g_{ox}, defined as follows: denoting e.g. by t^1 the integral of hopping between oxygen 1 and the Cu and by $t_{ox}^{1,2}$ the one between oxygens 1 and 2 (see figure 1), $g \equiv [\frac{\partial t^1}{\partial |\mathbf{r}_1|}]_0$ and $g_{ox} \equiv [\frac{\partial t_{ox}^{1,2}}{\partial |\mathbf{r}_1 - \mathbf{r}_2|}]_0$. We take $g < 0$ since a positive Cu–O hopping integral decreases as the Cu–O distance is increased. On the other hand, $g_{ox} > 0$, since physically the O–O hopping integral has the opposite sign with respect the Cu–O one. Following equations (3)–(6), the second-quantized electron–lattice Hamiltonian reads

$$H_{\mathrm{el-latt}}^{CuO_4} = \varepsilon_p \sum_{i,\sigma} n_{i,\sigma} + \varepsilon_d \sum_{\sigma} n_{d,\sigma} + \sum_{\eta} \hbar\omega_\eta b_\eta^\dagger b_\eta + t \sum_{i\sigma} (d_\sigma^\dagger p_{i\sigma} + \mathrm{h.c.}) + t_{ox} \sum_{i\sigma} (p_{i\sigma}^\dagger p_{i+1\sigma} + \mathrm{h.c.}) + U \left(\sum_i n_{i\uparrow}^{(p)} \hat{n}_{i\downarrow}^{(p)} + \hat{n}_\uparrow^{(d)} \hat{n}_\downarrow^{(d)} \right) + \sum_\eta \xi_\eta (b_\eta^\dagger + b_\eta) H_\eta, \tag{33}$$

where $p_{i\sigma}^\dagger$ and $p_{i\sigma}$ are the hole creation and annihilation operators on the oxygens $i = 1, \ldots, 4$ with spin $\sigma = \uparrow, \downarrow$, $d_\sigma^\dagger$ and d_σ are the hole creation and annihilation operators on the central copper site, while $n_{i\sigma}^{(p)} = p_{i\sigma}^\dagger p_{i\sigma}$ and $n_\sigma^{(d)} = d_\sigma^\dagger d_\sigma$ are the corresponding number operators. Henceforth we set $\varepsilon_p = \varepsilon_d = 0$ for convenience, since this simple choice is adequate for the present qualitative purposes. Also, we are assuming for simplicity that the oxygen–oxygen

[1] Some authors use an alternating sign convention for the bonds from a given Cu site. However, this is just a gauge; in the present CuO_4 case, this corresponds to changing the sign of two opposite oxygen orbitals. Even in the full plane, starting from positive t integrals, one can introduce staggered signs by negating a sublattice of O orbitals; then, one can arrange opposite signs for the bonds of each O by simply negating a sublattice of Cu. All this has no physical implications, and in our opinion does not help to visualize the real symmetry of the problem.

hopping t_{ox} is zero, and O–O hoppings are important only once the ions are moved. Similar results are obtained using a realistic t_{ox}, except that pair binding energies are somewhat reduced.

The H_η matrices are given by

$$
\begin{aligned}
H_{A_1} &= \frac{1}{2} g \sum_{i\sigma} (d^\dagger_\sigma p_{i\sigma} + \text{h.c.}) + \frac{1}{\sqrt{2}} g_{ox} \sum_{i\sigma} (p^\dagger_{i\sigma} p_{i+1\sigma} + \text{h.c.});\\
H_{A_2} &= 0;\\
H_{B_1} &= \tfrac{1}{2} g \sum_{\sigma} (d^\dagger_\sigma p_{1\sigma} - d^\dagger_\sigma p_{2\sigma} + d^\dagger_\sigma p_{3\sigma} - d^\dagger_\sigma p_{4\sigma} + \text{h.c.});\\
H_{B_2} &= \frac{1}{\sqrt{2}} g_{ox} \sum_{\sigma} (p^\dagger_{1\sigma} p_{2\sigma} - p^\dagger_{2\sigma} p_{3\sigma} + p^\dagger_{3\sigma} p_{4\sigma} - p^\dagger_{4\sigma} p_{1\sigma} + \text{h.c.});\\
H_{E_{1x}} &= \frac{1}{\sqrt{2}} g \sum_{\sigma} (-d^\dagger_\sigma p_{1\sigma} d^\dagger_\sigma p_{3\sigma} + \text{h.c.})\\
&\qquad + \tfrac{1}{2} g_{ox} \sum_{\sigma} (-p^\dagger_{1\sigma} p_{2\sigma} + p^\dagger_{2\sigma} p_{3\sigma} + p^\dagger_{3\sigma} p_{4\sigma} - p^\dagger_{4\sigma} p_{1\sigma} + \text{h.c.});\\
H_{E_{1y}} &= \frac{1}{\sqrt{2}} g \sum_{\sigma} (d^\dagger_\sigma p_{2\sigma} - d^\dagger_\sigma p_{4\sigma} + \text{h.c.})\\
&\qquad + \tfrac{1}{2} g_{ox} \sum_{\sigma} (p^\dagger_{1\sigma} p_{2\sigma} + p^\dagger_{2\sigma} p_{3\sigma} - p^\dagger_{3\sigma} p_{4\sigma} - p^\dagger_{4\sigma} p_{1\sigma} + \text{h.c.});\\
H_{E_{2x}} &= \tfrac{1}{2} g_{ox} \sum_{\sigma} (p^\dagger_{1\sigma} p_{2\sigma} - p^\dagger_{2\sigma} p_{3\sigma} - p^\dagger_{3\sigma} p_{4\sigma} + p^\dagger_{4\sigma} p_{1\sigma} + \text{h.c.});\\
H_{E_{2y}} &= \tfrac{1}{2} g_{ox} \sum_{\sigma} (-p^\dagger_{1\sigma} p_{2\sigma} - p^\dagger_{2\sigma} p_{3\sigma} + p^\dagger_{3\sigma} p_{4\sigma} + p^\dagger_{4\sigma} p_{1\sigma} + \text{h.c.}).
\end{aligned}
\tag{34}
$$

In order to make contact with the physics of cuprates, let us discuss the connection between the normal modes of the CuO_4 cluster and the phonon modes of the Cu–O planes. There is experimental evidence [15] that the possibly relevant modes for superconductivity lie on the CuO_2 planes and have a Cu–O bond stretching origin. In particular the LO *half-breathing* mode with $k = (\pi, 0), (0, \pi)$ is believed to couple significantly with the doped holes in the superconducting regime. In the CuO_4 cluster the half-breathing modes are contained in the breathing mode A_1 and in the quadrupolar mode B_1 by means of the linear combination $q_{A_1} \pm q_{B_1}$. We argue that qualitatively the effect of the coupling with the A_1 and B_1 modes should give us clues about the interplay between electronic $W = 0$ pairing and phonon exchange.

5. Lowest order effective interaction in CuO_4

The mere Hubbard CuO_4 cluster with O–O hopping $t_{ox} = 0$ yields [9] $\tilde{\Delta}(4) < 0$, due to a couple of degenerate $W = 0$ bound pairs, in the A_1 and B_2 irreps of the C_{4v} group; therefore in equation (28) we set the $m = m'$ labels accordingly. At weak coupling, we may simplify equation (28), neglecting all renormalizations; the phonon-mediated interaction for the B_2 pair reads

$$
\sum_{m'',q} \frac{V^q_{B_2,m''} V^q_{m'',B_2}}{E'_{m''} + \omega'_q - E} = -4 g^2_{ox} \frac{\lambda^2_{B_2}}{2\varepsilon_{A_1} + \omega_{B_2} - E}. \tag{35}
$$

Note that, in the denominator in the rhs, $2\varepsilon_{A_1} + \omega_{B_2}$ is the energy of an unrenormalized excited $|m\rangle \otimes |q\rangle\rangle$ state, which at weak coupling is higher than the ground state energy E; hence the rhs must be negative and the B_2 phonon is synergetic with electronic pairing. On the other

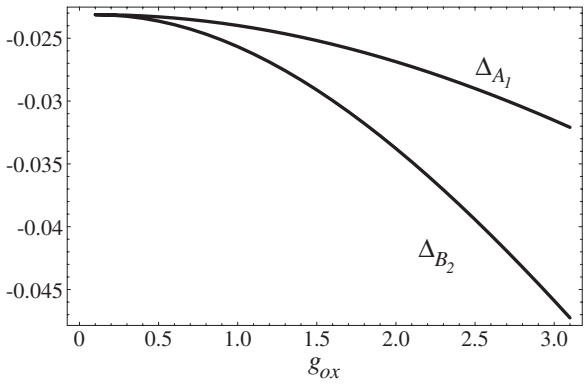

Figure 2. Analytical results of the canonical transformation: pair binding energy in the A_1 and B_2 sectors as a function of g_{ox}. Here we used $\lambda_\eta = 1$ for every mode, $t = 1$ eV, $t_{ox} = 0$, $U = 1$ eV; g_{ox} is in units of $\varepsilon_0/\xi_0 = 1$ eV Å^{-1}, Δ is in eV.

hand, the vibronic effective interaction for the A_1 pair is

$$\sum_{m'',q} \frac{V^q_{A_1,m''} V^q_{m'',A_1}}{E_{m''} + \omega'_q - E} = -\frac{4}{3} g^2_{ox} \left(\frac{\lambda^2_{B_2}}{2\varepsilon_{A_1} + \omega_{B_2} - E} + \frac{2\lambda^2_{A_1}}{2\varepsilon_{A_1} + \omega_{A_1} - E} - \frac{\lambda^2_{E_1}}{2\varepsilon_{A_1} + \omega_{E_1} - E} - \frac{\lambda^2_{E_2}}{2\varepsilon_{A_1} + \omega_{E_2} - E} \right). \tag{36}$$

This shows that in the A_1 sector the total sign depends on the relative weight of attractive and repulsive contributions. Equations (35), (36) show that at weak coupling A_1 and B_2 modes are synergetic to the $W = 0$ pairing, while both longitudinal and transverse E modes are pair breaking. The half-breathing modes that are deemed most important [15, 16] are $A_1 \pm B_1$ combinations, but B_1 does not appear in equations (35), (36). The numerical calculations reported below confirm these findings over a broad range of parameters.

For the sake of argument, in the explicit calculations we took all the normal modes with the same energy $\varepsilon_0 = \hbar\omega_0 = 10^{-1}$ eV and $\lambda_\eta = 1$. This sets the length scale of lattice effects $\xi_0 = \sqrt{\frac{\hbar}{2M\omega_0}} \simeq 10^{-1}$ Å where we used $M = 2.7 \times 10^{-26}$ kg for oxygen.

With this choice, the Cooper-like equation (25) reads

$$(2\varepsilon_{A_1} - E) - \frac{U^2}{16} \left(\frac{1}{\varepsilon_{B_1} + \varepsilon_{A_1} - E} - \frac{1}{2} \frac{1}{\varepsilon_{A_1} + \varepsilon_{A'_1} - E} \right) - \frac{4}{3} g^2_{ox} \frac{1}{2\varepsilon_{A_1} + \omega_0 - E} = 0 \tag{37}$$

in the A_1 channel and

$$(2\varepsilon_{A_1} - E) - \frac{U^2}{16} \left(\frac{1}{\varepsilon_{B_1} + \varepsilon_{A_1} - E} - \frac{1}{2} \frac{1}{\varepsilon_{A_1} + \varepsilon_{A'_1} - E} \right) - 4 g^2_{ox} \frac{1}{2\varepsilon_{A_1} + \omega_0 - E} = 0 \tag{38}$$

for B_2 pairs. The eigenvalue E, like in equation (8), is the total energy of the cluster; it must be compared with the threshold $E^{(R)}_T$ of equation (31), whose noninteracting limit is $E^{(R)}_T = 2\varepsilon_{A_1}$ since the degenerate level energy (see table A.2, appendix A) is $\varepsilon_p = 0$. It turns out that using equation (32) in the weak coupling approximation, that ignores renormalizations, the effective interaction is $\Delta = E - 2\varepsilon_{A_1}$; in appendix B we verify by perturbation theory that, like in the Hubbard model, $\Delta = \tilde{\Delta}(4)$; this supports our interpretation of $\tilde{\Delta}$ as minus the pairing energy.

The trends of Δ in both channels are shown in figure 2. The vibrations split the degeneracy of the $W = 0$ pairs, effectively lowering the symmetry like a nonvanishing t_{ox}. Pairing is

enhanced in the A_1 sector as well, albeit less than in B_2; without phonons, $\Delta \simeq -20$ meV for both the $W = 0$ pairs.

6. Jahn–Teller mixing of electronic ground states and pairing

If the inclusion of the lattice degrees of freedom really systematically leads to $\tilde{\Delta} > 0$, purely electronic cluster models become totally irrelevant to superconductivity, as was argued [18]. However small, the CuO_4 cluster yields electronic pairing and allows one to test this important point.

In this section we set up a conventional calculation of the JT effect involving degenerate electronic ground states and their mixing with the vibrations. We first take the nuclei as frozen in a C_{4v}-symmetric configuration and diagonalize the purely electronic part of the Hamiltonian:

$$H_{\rm el}^{\rm CuO_4} = t \sum_{i\sigma} (d_\sigma^\dagger p_{i\sigma} + \text{h.c.}) + U \left(\sum_i n_{i\uparrow}^{(\rm p)} n_{i\downarrow}^{(\rm p)} + n_\uparrow^{(\rm d)} n_\downarrow^{(\rm d)} \right). \tag{39}$$

As before, we are using $t_{\rm ox} = \varepsilon_p = \varepsilon_d = 0$.

The JT effect arises if the ground state of $H_{\rm el}^{\rm CuO_4}$ is degenerate, with a ground state multiplet $\{|\Psi_1\rangle, \ldots, |\Psi_n\rangle\}$ such that $H_{\rm el}^{\rm CuO_4}|\Psi_k\rangle = {\rm E}_0|\Psi_k\rangle$. If we take matrix elements of $H_{\rm el-latt}^{\rm CuO_4}$ in this truncated (n-dimensional) electronic basis, integrating over electrons and keeping boson operators, we get the *dynamical* JT Hamiltonian [29, 30], with matrix elements

$$H_{\alpha,\beta}^{\rm JT} = \left({\rm E}_0 + \sum_\eta \hbar\omega_\eta b_\eta^\dagger b_\eta \right) \delta_{\alpha,\beta} + \langle \Psi_\alpha | V | \Psi_\beta \rangle. \tag{40}$$

It is worth noting that neglecting the nuclear kinetic energy (i.e. $-\frac{\hbar^2}{2M} \sum_i \frac{\partial^2}{\partial^2 \mathbf{r}_i} \to 0$) and treating the nuclear positions as variational parameters corresponds to the *static* JT Hamiltonian, but we follow the dynamic treatment which is superior.

In the following we assume that the initial configuration is stable with respect to the mode A_1 which only changes the scale of the CuO_4 molecule. Since this mode does not produce any JT distortion, it is not involved in the arguments of [18]. In this section, we study $\tilde{\Delta}(4)$ in this approximation, according to equation (1). The ground state with two holes is a nondegenerate totally symmetric singlet unaffected by the JT effect; in the other cases, the use of the Hamiltonian (40) is justified provided that the excited states are several phonon energies above the ground state.

6.1. Three-hole ground state mixing

With three holes the ground state belongs to the three-dimensional irrep of S_4 which in C_{4v} breaks into $B_1 \oplus E$. To illustrate the electronic structure and its dependence on distortions, in figure 3 we show the adiabatic potential energy surface projected along the B_2 distortion. Projecting on the other directions, we obtain similar trends. It is clear that the ground state multiplet is well separated from the excited states and hence this treatment of the JT effect is well justified.

Since $E \otimes E$ contains all the irreps of C_{4v}, all the normal modes are JT active in this case. Following equation (40), we computed the following V matrix elements in the three-hole ground state multiplet with the Hubbard interaction, using equation (34). The four independent elements at the optimal value $U/t \sim 5$, where the $W = 0$ pair binding energy is maximum, are

$$\gamma_1 = \langle \Psi_{\rm B_1} | H_{\rm E_{1x}} | \Psi_{\rm E_x} \rangle = 0.17 g_{\rm ox}, \tag{41}$$

$$\gamma_2 = \langle \Psi_{\rm B_1} | H_{\rm E_{2y}} | \Psi_{\rm E_x} \rangle = 0.24 g + 0.17 g_{\rm ox}, \tag{42}$$

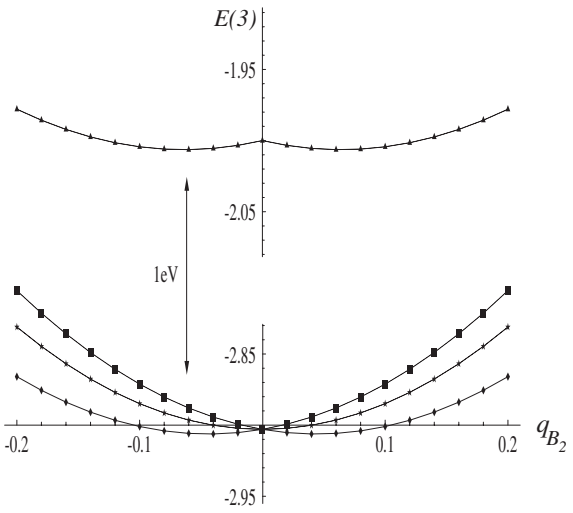

Figure 3. Adiabatic potential energy surfaces along B_2 for the ground and first excited three-hole states of CuO_4. Here, q_{B_2} denotes the classical normal coordinate; $U = 5$ eV, $t = 1$ eV, $g = -2.4$, $g_{ox} = 0.6$ in units eV Å^{-1}, and $\omega_\eta = 0.1$ eV $\forall\eta$; the displacement q_{B_2} is in Å, energies are in eV. The ground state multiplet is below the first excited state by $\sim$1 eV.

$$\gamma_3 = \langle \Psi_{E_x} | H_{B_1} | \Psi_{E_x} \rangle = 0.24g, \tag{43}$$

$$\gamma_4 = \langle \Psi_{E_y} | H_{B_2} | \Psi_{E_x} \rangle = -1.05 g_{ox}. \tag{44}$$

The JT Hamiltonian reads

$$H_{JT}(3) = \left[E_0(3) + \sum_\eta \hbar\omega_\eta b_\eta^\dagger b_\eta \right] \otimes \mathbf{1}_{3\times 3} + \sum_\eta \xi_\eta (b_\eta^\dagger + b_\eta) M_\eta, \tag{45}$$

where $E_0(3)$ is the ground state energy of $H_{el}^{CuO_4}$ with three holes and

$$M_{B_1} = \gamma_3 \begin{pmatrix} 0 & 0 & 0 \\ 0 & 1 & 0 \\ 0 & 0 & -1 \end{pmatrix}, \tag{46}$$

$$M_{B_2} = \gamma_4 \begin{pmatrix} 0 & 0 & 0 \\ 0 & 0 & 1 \\ 0 & 1 & 0 \end{pmatrix}, \tag{47}$$

$$M_{E_{1x}} = \begin{pmatrix} 0 & \gamma_2 & -\gamma_1 \\ \gamma_2 & 0 & 0 \\ -\gamma_1 & 0 & 0 \end{pmatrix}, \tag{48}$$

$$M_{E_{1y}} = \begin{pmatrix} 0 & -\gamma_1 & -\gamma_2 \\ -\gamma_1 & 0 & 0 \\ -\gamma_2 & 0 & 0 \end{pmatrix}, \tag{49}$$

$$M_{E_{2x}} = \gamma_1 \begin{pmatrix} 0 & -1 & 1 \\ -1 & 0 & 0 \\ 1 & 0 & 0 \end{pmatrix}, \tag{50}$$

and

$$M_{E_{2y}} = \gamma_1 \begin{pmatrix} 0 & 1 & 1 \\ 1 & 0 & 0 \\ 1 & 0 & 0 \end{pmatrix}. \tag{51}$$

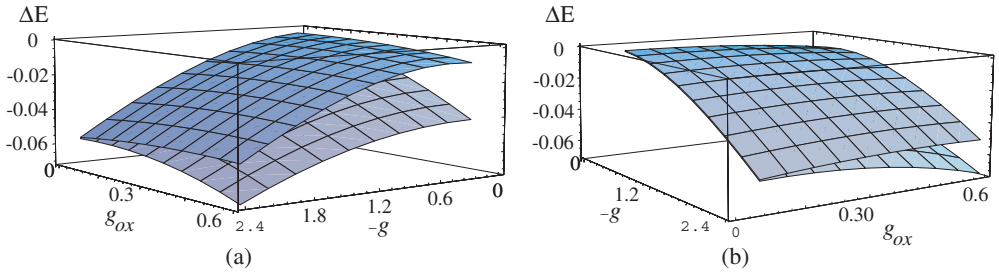

Figure 4. (a) The vibronic correction ΔE to $E_0(3)$ for the E state (lower surface) and the B_1 state (upper one) as a function of g and g_{ox}. (b) The same surfaces from another point of view. Here, $t = 1$ eV, $U = 5$ eV, ΔE is in eV and $\hbar\omega = 0.1$ eV, g and g_{ox} are in units of $\varepsilon_0/\xi_0 = 1$ eV Å^{-1}.

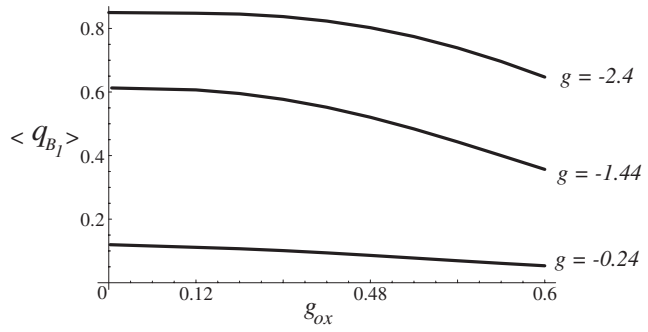

Figure 5. $\langle \hat{q}_{B_1} \rangle$ as a function of $-g$ and g_{ox}. Here $t = 1$ eV, $U = 5$ eV, $\langle \hat{q}_{B_1} \rangle$ is in units of ξ_0, g and g_{ox} are in units of $\varepsilon_0/\xi_0 = 1$ eV Å^{-1}.

We numerically diagonalized $H_{JT}(3)$ in the Hilbert space spanned by $|\Psi_\eta\rangle \otimes |\Phi_{N_{ph}}\rangle$, where $\eta = B_1, E_x, E_y$ is the electronic state and $|\Phi_{N_{ph}}\rangle$ is a vibration state in the truncated Hilbert space with all modes having vibrational quantum numbers $\leqslant N_{ph}$. Excluding the breathing mode the size of the problem is $3(N_{ph} + 1)^6$. We consider $N_{ph} = 3$, since already in the weak coupling regime $\tilde{\Delta}$ changes sign. We studied $\omega_\eta = \omega = 0.1$ eV, $\lambda_\eta = 1\ \forall\eta$ in the range of $|g|$ and $|g_{ox}|$ between 0 and 2.4 eV Å^{-1}, which means that the number ratios $|\gamma_i|\sqrt{\frac{\hbar}{2M\omega}}/\hbar\omega$ vary between 0 and 0.5. This weak coupling condition ensures that $N_{ph} = 3$ is indeed adequate. The results are shown in figure 4.

The lower surface represents the ground state energy shift ΔE for electronic states belonging to the degenerate irrep E, while the higher one is ΔE for the B_1 state. The JT effect partially removes the threefold degeneracy and the ground state is an E doublet. Note that according to the textbook, static JT effect, one should observe a total removal of the degeneracy. This is however not borne out by the dynamical calculation and, for $g_{ox} = 0$, all three states remain degenerate (see figure 4(b)).

The way the system dynamically distorts is also of interest. The only vibration having a coordinate on the diagonal of $H_{JT}(3)$ is B_1; thus, the E doublet can only distort along the B_1 normal mode. In other words, with $\hat{q}_{B_1} = \xi_{B_1}(b^\dagger_{B_1} + b_{B_1})$, $\langle \hat{q}_{B_1} \rangle \equiv \langle \Psi^0_{E_x} | \hat{q}_{B_1} | \Psi^0_{E_x} \rangle = -\langle \Psi^0_{E_y} | \hat{q}_{B_1} | \Psi^0_{E_y} \rangle \neq 0$. The trend of $\langle \hat{q}_{B_1} \rangle$ as a function of g and g_{ox} is shown in figure 5. We observe that $\langle \hat{q}_{B_1} \rangle \to 0$ as $g \to 0$; we also remark that the deformation depends essentially by g and only weakly on g_{ox} because according to equation (43) the coupling constant γ_3 responsible for the distortion along B_1 depends on g and not on g_{ox}. The E–B_1 splitting, in contrast, depends on g_{ox} and only weakly on g. The naive expectation that splittings accompany distortions only holds for static ones.

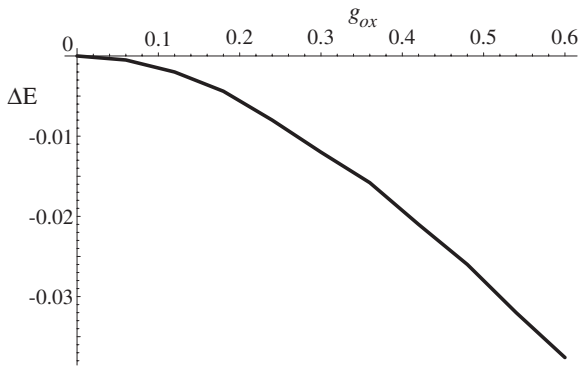

Figure 6. The ground state energy shift ΔE as a function of $g_{\rm ox}$. Here $t = 1$ eV, $U = 5$ eV, ΔE is in eV, $g_{\rm ox}$ is in units of $\varepsilon_0/\xi_0 = 1$ eV Å^{-1}, $\lambda_{\rm B_2} = 1$, $\omega_{\rm B_2} = 0.1$ eV.

6.2. Four-hole ground state mixing

With four holes, $H_{\rm el}^{\rm CuO_4}$ has a twofold-degenerate ground state; it belongs to the two-dimensional irrep of S_4 that breaks in $\rm A_1 \oplus B_2$ in $\rm C_{4v}$. Thus, the only JT-active mode is $\rm B_2$, which makes the problem exactly resolvable in terms of a continued fraction [31].

Following again equations (40), the second-quantized JT Hamiltonian with four particles reads

$$H_{\rm JT}(4) = [\hbar\omega_{\rm B_2} b^\dagger_{\rm B_2} b_{\rm B_2} + E_0(4)] \otimes \mathbf{1}_{2\times 2} + \xi_{\rm B_2}\gamma_5 (b^\dagger_{\rm B_2} + b_{\rm B_2}) \begin{pmatrix} 0 & 1 \\ 1 & 0 \end{pmatrix}. \qquad (52)$$

in the space spanned by the electronic ground states. The coupling constant γ_5 is given by

$$\gamma_5 = \langle \Psi_{\rm A_1} | H_{\rm B_2} | \Psi_{\rm B_2} \rangle = 1.19 g_{\rm ox}, \qquad (53)$$

where, as usual, the matrix element in equation (53) is evaluated at $U/t \sim 5$.

The ground state energy of $H_{\rm JT}(4)$ in the sector of symmetry η coincides with the lowest pole of the Green function:

$$\begin{aligned} G_{\eta,\eta}(E) &= \langle\langle 0| \otimes \langle \Psi_\eta | \frac{1}{E - H_{\rm JT}(4) + {\rm i}0^+} |\Psi_\eta\rangle \otimes |0\rangle\rangle \\ &= \cfrac{1}{\chi(0) - \cfrac{(\xi_{\rm B_2}\gamma_5)^2}{\chi(1) - \cfrac{3(\xi_{\rm B_2}\gamma_5)^2}{\chi(2) - \cfrac{5(\xi_{\rm B_2}\gamma_5)^2}{\chi(3) - \cfrac{7(\xi_{\rm B_2}\gamma_5)^2}{\chi(4) - \cdots}}}}}, \end{aligned} \qquad (54)$$

where $\eta = \rm A_1, B_2$ and $\chi(n) = E - E_0(4) - n\hbar\omega_{\rm B_2}$. $G_{\eta,\eta}(E)$ does not depend on η and the energy corrections in the $\rm A_1$ and $\rm B_2$ sectors are the same. The ground state energy shift ΔE as a function of $g_{\rm ox}$ is plotted in figure 6.

There are no diagonal couplings in equation (52), which implies no distortions; the energy correction is much smaller than in the three-hole case.

In figure 7 we show the adiabatic potential curve, with the same parameters as in figure 7. In contrast with the three-hole case, the ground state multiplet is separated from the excited states by ∼100–150 meV which is comparable with the phonon energies. Hence we expect, in this case, the approximation restricting the Hilbert space to the lowest multiplet not to be justified. However, in the case of weak coupling to soft vibrations, with ω small compared to the gap in the electronic spectrum, this approximation should work well.

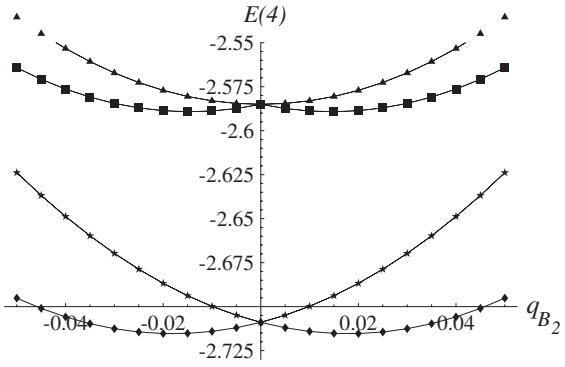

Figure 7. The adiabatic potential energy curve for the low lying four-hole states of CuO_4. Here, q_{B_2} denotes the classical normal coordinate; $U = 5$ eV, $t = 1$ eV, $g = -2.4$, $g_{ox} = 0.6$ eV Å^{-1}, and $\frac{1}{2}M\omega_{B_2}^2 = 20$ eV Å^{-2}; the displacement is in Å, energies are in eV. The ground state multiplet is below the first excited state by ∼100–150 meV which is of the order of $2|\tilde{\Delta}|$.

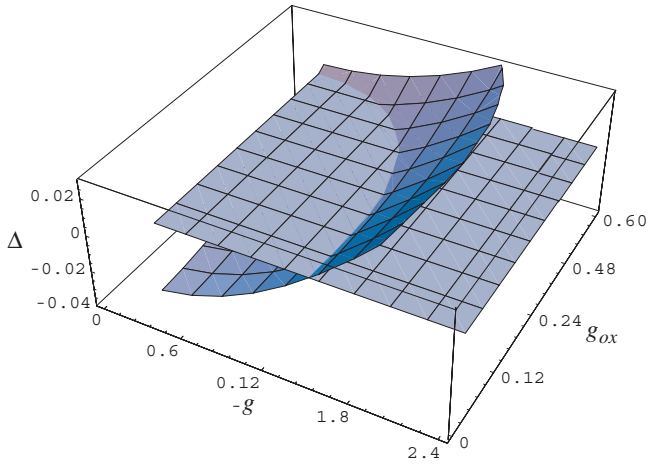

Figure 8. $\tilde{\Delta}$ as a function of $-g$ and g_{ox}, according to the theory of the present section. $\tilde{\Delta}$ is in eV, g and g_{ox} are in units of $\varepsilon_0/\xi_0 = 1$ eV Å^{-1}. Here $t = 1$ eV, $U = 5$ eV, $\omega_{B_2} = 0.1$ eV.

6.3. $W = 0$ pairing in the presence of Jahn–Teller distortions

Collecting together the results of the present section we obtain the behaviour of $\tilde{\Delta}$ in a popular approximation that neglects the excited electronic states. In figure 8 we show the plot of $\tilde{\Delta}$ as a function of $-g$ and g_{ox}, shown with the zero-energy plane. The maximum distortion along B_1 compatible with $\tilde{\Delta} < 0$ (see figure 8) is $\langle q_{B_1}^{max} \rangle \simeq 3 \times 10^{-2}$ Å, which is attained at $g \simeq 1$ eV × Å^{-1} and $g_{ox} = 0$.

Both the system with four holes and that with three holes gain energy by the JT effect; $\tilde{\Delta}$ remains negative only in the weak EP coupling regime, since the decrease of $2E(3)$ overcomes the decrease of $E(4)$. This is due to the fact that the system with three holes can gain energy by mixing with $B_1, B_2, E_{1x}, E_{1y}, E_{2x}, E_{2y}$ vibrations, while the system with four holes can do it only with the B_2 mode. Moreover, the factor 2 in front of $E(3)$ in the expression for $\tilde{\Delta}$ further favours the distortion in the three-hole case.

These results, in line with [18], would imply that the electronic pairing is limited to relatively weak EP couplings and that at any rate the vibrations are invariably detrimental to $W = 0$ pairing. However, we know from section 5 that this conclusion is remarkably but

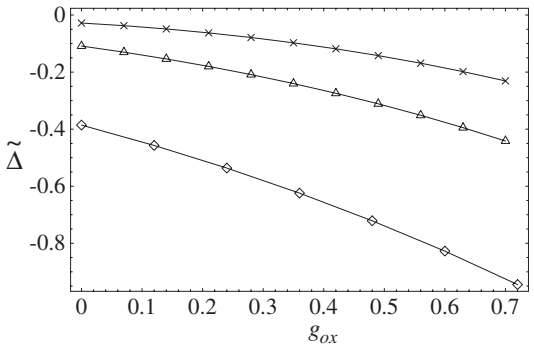

Figure 9. Exact diagonalization results for $\tilde{\Delta}(4)$ in eV, with only the A_1 phonon active, $N_{ph} = 20$, as a function of g_{ox} for different values of g: $g = -0.2$ (crosses); $g = -0.5$ (triangles); $g = -1$ (diamonds). Here we used $t = 1$ eV, $t_{ox} = 0$, $U = 1$ eV; g_{ox} and g are in units of $\varepsilon_0/\xi_0 = 1$ eV Å^{-1}.

definitely wrong, because the full theory predicts synergy of vibrations and $W = 0$ pairing at least at weak coupling. This failure of the JT Hamiltonian is due to the neglect of the electronic excited states, causing a severe overestimation of the four-hole energy. The physical reason is that if we restrict the mixing to the degenerate states the electronic wavefunction is too rigid. On the other hand, including all the multiplet of states arising from the degenerate one-electron level, the pair can achieve the flexibility which allows it to follow adiabatically the vibration-induced deformations, as we shall see in the next section.

Detecting the failure of a textbook procedure is in itself a potentially very interesting result; it is a merit of a relatively simple model like this that it allows one to understand in detail how this arises.

7. Numerical results of the full theory

Since the conventional JT Hamiltonian is not enough, to see what really happens in this model with increasing EP coupling, where the analytic treatment of section 5 loses validity, we resort to numerical methods. In this section we explore the pairing scenario numerically, which offers an independent check of the weak coupling calculations and permits one to go beyond the weak coupling regime. First, we analyse one phonon at a time ($\lambda_\eta = 1$), turning off the all others ($\lambda_\eta = 0$); $\omega_\eta \equiv 0.1$ for all modes. In this way we see which kind of phonon is cooperative with the $W = 0$ pairing and which is not. We have performed these calculations in a virtually exact way, by including a number of phonons N_{ph} up to 20. To this end we take advantage of the recently proposed *spin-disentangled* diagonalization technique [11]. The results are shown in figures 9–11.

The plots show the trend of $\tilde{\Delta}(4)$ as a function of g_{ox} and g. It appears (see figures 9 and 10) that if g_{ox} is increased, the A_1 and B_2 phonons enhance the pairing, even beyond the weak coupling regime. The further enhancement of $|\tilde{\Delta}(4)|$ due to A_1 as $|g|$ is increased is not predicted by the weak coupling theory (equation (36)). The B_1 phonon is slightly suppressive, but it affects the pairing energy on a scale of 10^{-5} eV and hence its contribution is negligible. On the other hand, the (longitudinal and transverse) E phonons (see figures 10 and 11) have an unambiguous tendency to destroy the pairing. In particular, the E_1 mode does it both by increasing g_{ox} and by increasing $|g|$.

The results presented show that the behaviour of the individual phonons is essentially the same as predicted analytically in section 5: some of them (A_1 and B_2) act in a cooperative

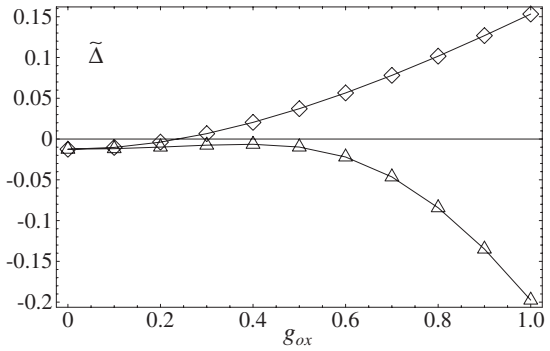

Figure 10. Exact diagonalization results for $\tilde{\Delta}(4)$ in eV, with only one phonon active, B_2 (triangles) or E_2 (diamonds), $N_{\rm ph} = 20$. Here we used $t = 1$ eV, $U = 1$ eV; $g_{\rm ox}$ and g are in units of $\varepsilon_0/\xi_0 = 1$ eV Å^{-1}.

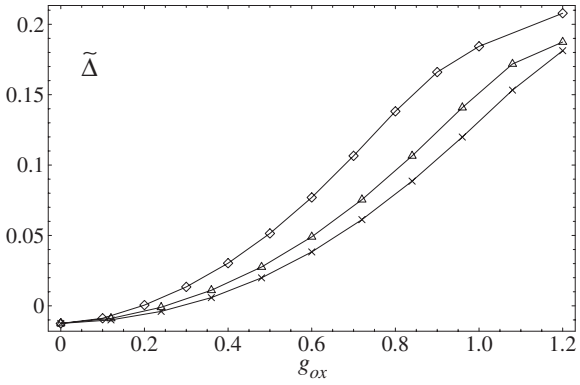

Figure 11. Exact diagonalization results for $\tilde{\Delta}(4)$ in eV, with only the E_1 phonon active, $N_{\rm ph} = 20$, as a function of $g_{\rm ox}$ for different values of g: $g = -0.2$ (crosses); $g = -0.5$ (triangles); $g = -1$ (diamonds). Here we used $t = 1$ eV, $t_{\rm ox} = 0$, $U = 1$ eV; $g_{\rm ox}$ and g are in units of $\varepsilon_0/\xi_0 = 1$ eV Å^{-1}.

way with the electronic pairing mechanism; some others (E phonons) do not; the B_1 mode is quite inactive. However, for a proper understanding of the conflicting vibronic effects we need to include as many phonon modes as possible at the same time. In this case the exact diagonalizations become hard even with a modest $N_{\rm ph}$ per vibration. We performed exact diagonalizations of $H^{\rm CuO_4}_{\rm el-latt}$ with five active modes; with five holes, the size of the problem is $100(N_{\rm ph} + 1)^5$; we could afford $N_{\rm ph} = 3$ for each. Some results are shown in figure 12.

In figure 12(a) we included the vibrations with $\eta = A_1, B_1, B_2, E_{2x}, E_{2y}$; one notes a strong, monotonic increase of the binding energy with both $g_{\rm ox}$ and $|g|$. The weak coupling theory of section 5 qualitatively explains the $g_{\rm ox}$ dependence but not the $|g|$ one: when the EP coupling gets strong, the Cu–O stretching becomes important. In figure 10 (diamonds) we noted that the E_2 vibrations alone tend to destroy pairing; here we observe that when they compete with A_1 and B_2 their effects are utterly suppressed. It is possible that the couplings to the pair breaking E modes are somewhat underestimated due to the choice of λ parameters.

In figure 12(b) we included the vibrations with $\eta = A_1, B_1, B_2, E_{1x}, E_{1y}$, and we observe that $\tilde{\Delta}$ now becomes positive at moderate $g_{\rm ox}$. Comparing with the above results on individual modes, we observe that in going from figures 12(a), (b) we are replacing the pair breaking transverse E_2 phonons by the pair breaking, longitudinal E_1 modes. We conclude that the

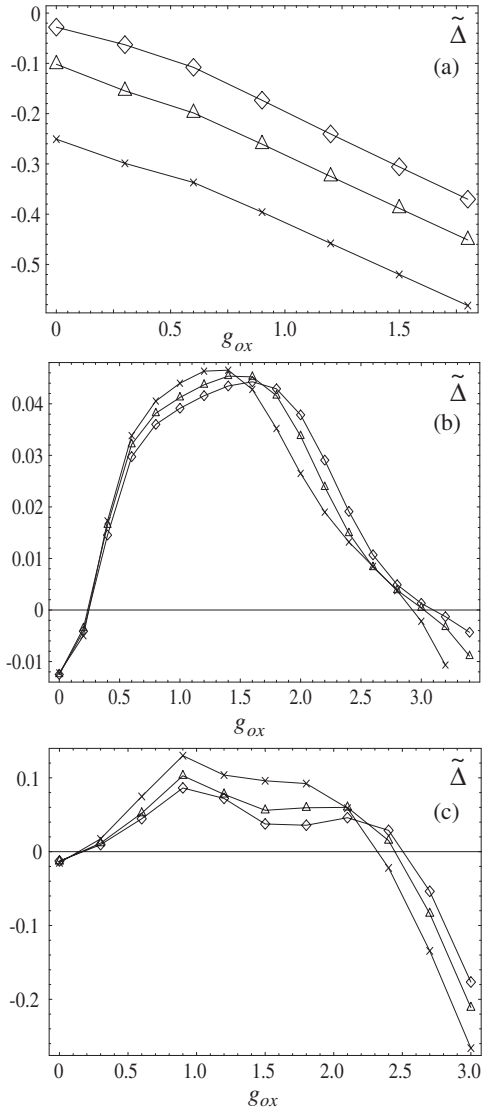

Figure 12. $\tilde{\Delta}(4)$ in eV as a function of $g_{\rm ox}$ for different values of g. $\lambda_\eta = 1$ for all the vibrations, except: $\lambda_\eta = 0$ for $\eta = {\rm E}_1$ (a); $\lambda_\eta = 0$ for $\eta = {\rm E}_2$ (b); $\lambda_\eta = 0$ for $\eta = {\rm A}_1, {\rm B}_2$ (c). $N_{\rm ph} = 3$ for each active mode; $g = -0.2$ (diamonds); $g = -0.5$ (triangles); $g = -1$ (crosses). Here we used $t = 1$ eV, $t_{\rm ox} = 0$, $U = 1$ eV; $g_{\rm ox}$ and g are in units of $\varepsilon_0/\xi_0 = 1$ eV Å^{-1}.

longitudinal ones are more efficient in restoring the repulsion and at intermediate coupling they overwhelm the pair healing A_1 and B_2.

However, for $g_{\rm ox} \gtrsim 0.15$ eV Å^{-1}, the cooperative modes prevail and $\tilde{\Delta}(4)$ becomes negative again. This remarkable behaviour could not be anticipated from the weak coupling approach of section 5, where only the one-phonon exchange diagrams were included as in the BCS theory.

In figure 12(c) the active modes are $\eta = {\rm B}_1, {\rm E}_{1x}, {\rm E}_{1y}, {\rm E}_{2x}, {\rm E}_{2y}$; these are all pair breaking individually and, switching them together, they readily unbind pairs, leading to strong positive $\tilde{\Delta}$. However, unexpectedly, we again find attraction at large enough $g_{\rm ox}$.

It is likely that the couplings to the pair breaking E modes are somewhat overestimated due to the choice of λ parameters in figures 12(b) and (c). The pairing at strong coupling observed in figures 12(b) and (c) results from more complicated interactions leading to bipolaron formation. This recalls the charge-ordered superlattice phase found in [25]; however, they used a Hubbard–Holstein model and, since the system is one dimensional, the electronic pairing does not occur in their case.

8. Conclusions

Introducing vibrations and vibronic couplings into a strongly correlated model opens up a rich scenario where, among other possibilities, pairing can be achieved by a synergy of electronic correlation and phonon exchange. A possible outcome, however, is competition among different symmetry vibration modes and electronic excitations. We illustrate the situation by using a CuO_4 model that allows a full treatment of all degrees of freedom and hosts bound $W = 0$ pairs when undistorted, has vibrations of the same symmetries as the CuO plane, and is numerically affordable. A popular recipe for computing JT distorted molecules prescribes restricting to the degenerate electronic levels, letting them interact with the JT-active modes. A static treatment invariably leads to a complete removal of the symmetry and a nondegenerate ground state. We put forward a fuller dynamical theory which partly preserves the degeneracy; however, the vibrations are always opposing $W = 0$ pairing which is thereby reduced to a weak EP coupling effect. This restricted basis, however, may only be valid provided that the excited states of the unperturbed electronic Hamiltonian are far removed from the ground state on the energy scale set by the frequency of the relevant phonon modes. With the cuprates in mind, we consider a situation where the phonon energies and the superconducting gap are comparable, in the 0.1 eV range; we diagonalize the full model keeping up to five simultaneous modes and vibrational quantum numbers $N_{\rm ph} \leqslant 3$. Depending on the parameters, a rich phenomenology emerges from the numerical data. Pairing prevails at weak EP coupling, as expected, but the phonon contributions which dominate in such a case turn out to contribute to the pairing rather than opposing it. The correct trend is predicted by a canonical transformation approach, which also explains the pairing or pair breaking character of the modes. In particular it is found that the half-breathing modes give a synergetic contribution to the purely electronic pairing; since they are believed to be mainly involved in optimally doped cuprates, our findings suggest a joint mechanism, with a Hubbard model that captures a crucial part of the physics.

This agreement validates the canonical transformation approach, which allows one to carry out useful calculations even in large systems that do not lend themselves to exact diagonalization.

At intermediate coupling the outcome of the theory depends essentially on the relative weight of the coupling to the longitudinal and transverse vector modes, which destabilize pairing most effectively.

Remarkably, however, the vibrations restore pairing again at strong coupling, when a bipolaronic regime prevails. This scenario was also derived in the context of an extended t–J model, where the half-breathing mode was found to enhance electronic pairing [17, 32].

Finally, experimental data on nanopowders [33] also indicate that one should not be overly pessimistic about cluster calculations. The pairing that shows up there can be relevant and provide physical insight concerning the interplay of various degrees of freedom for pair structure and formation.

Acknowledgments

We thank Gianluca Stefanucci and Agnese Callegari for useful discussions.

Table A.1. The character table of the C_{4v} symmetry group. Here **1** denotes the identity, C_2 the 180° rotation, $C_4^{(+)}$, $C_4^{(-)}$ the anticlockwise and clockwise 90° rotations, σ_x, σ_y the reflections with respect to the $y = 0$ and $x = 0$ axes, and σ_+, σ_- the reflections with respect to the $x = y$ and $x = -y$ diagonals. In the last column we show typical basis functions.

C_{4v}	**1**	C_2	$C_4^{(+)}$, $C_4^{(-)}$	σ_x, σ_y	σ_+, σ_-	Symmetry
A_1	1	1	1	1	1	$x^2 + y^2$
A_2	1	1	1	−1	−1	$(x/y) - (y/x)$
B_1	1	1	−1	1	−1	$x^2 - y^2$
B_2	1	1	−1	−1	1	xy
E	2	−2	0	0	0	(x, y)

Table A.2. One-body levels of the CuO_4 cluster in units of t; the last line reports the values for $t_{ox} = 0$ which are used in the text.

$\frac{\varepsilon_{A_1}}{t}$	$\frac{\varepsilon_{B_1}}{t}$	$\frac{\varepsilon_{E_x}}{t}$	$\frac{\varepsilon_{E_y}}{t}$	$\frac{\varepsilon_{A_1'}}{t}$
$\tau - \sqrt{4+\tau^2}$	-2τ	0	0	$\tau + \sqrt{4+\tau^2}$
−2	0	0	0	2

Appendix A. $W = 0$ pairs in the CuO_4 cluster

The CuO_4 Hubbard Hamiltonian has C_{4v} symmetry. When the oxygen–oxygen hopping is absent, the symmetry group is the permutation group S_4, and although for convenience we continue to use the subgroup C_{4v} labels, it is S_4 that must be used for the $W = 0$ theorem [12]. The character table appears as table A.1.

Setting for simplicity $\varepsilon_d = \varepsilon_p = 0$, the one-body spectrum of the CuO_4 Hamiltonian has the eigenvalues given in table A.2.

Here we label the eigenvalues with the irreps of the corresponding eigenfunctions. The level energies are in units of t, $\tau \equiv t_{ox}/t$; for $t_{ox} = 0$, $\varepsilon_{E_x} = \varepsilon_{E_y} = \varepsilon_{B_1} = 0$. The corresponding one-body creation operators for a particle in each of these eigenstates are

$$c^\dagger_{E_y\sigma} = \frac{1}{\sqrt{2}}(p^\dagger_{2\sigma} - p^\dagger_{4\sigma}), \tag{55}$$

$$c^\dagger_{E_x\sigma} = \frac{1}{\sqrt{2}}(p^\dagger_{1\sigma} - p^\dagger_{3\sigma}), \tag{56}$$

$$c^\dagger_{B_1\sigma} = \tfrac{1}{2}(p^\dagger_{1\sigma} - p^\dagger_{2\sigma} + p^\dagger_{3\sigma} - p^\dagger_{4\sigma}), \tag{57}$$

$$c^\dagger_{A_1\sigma}(1) = \frac{1}{\alpha^2+4}(\alpha d^\dagger_\sigma + p^\dagger_{1\sigma} + p^\dagger_{2\sigma} + p^\dagger_{3\sigma} + p^\dagger_{4\sigma}), \tag{58}$$

$$c^\dagger_{A_1\sigma}(2) = \frac{1}{\beta^2+4}(\beta d^\dagger_\sigma + p^\dagger_{1\sigma} + p^\dagger_{2\sigma} + p^\dagger_{3\sigma} + p^\dagger_{4\sigma}), \tag{59}$$

where α and β depend on τ as follows:

$$\alpha = \frac{4\left(-1 - \tau^2 + \tau\sqrt{4+\tau^2}\right)}{-5\tau - 2\tau^3 + \sqrt{4+\tau^2} + 2\tau^2\sqrt{4+\tau^2}}, \tag{60}$$

$$\beta = \frac{4\left(1 + \tau^2 + \tau\sqrt{4+\tau^2}\right)}{5\tau + 2\tau^3 + \sqrt{4+\tau^2} + 2\tau^2\sqrt{4+\tau^2}}. \tag{61}$$

By the $W = 0$ theorem [12], the irrep $A_1 \oplus B_2$ of the group S_4 which is not represented in the one-body spectrum must yield singlet eigenstates with no double occupation. Projecting, one

Table B.1. Shorthand notation used in equations (63)–(65).

$\frac{1}{d_1} = -\varepsilon_{A_1} + \varepsilon_{A_1'}$	$\frac{1}{d_2} = -\varepsilon_{A_1} + \omega_{B_1}$	$\frac{1}{d_3} = -\varepsilon_{A_1} + \omega_{E_1}$
$\frac{1}{d_4} = -\varepsilon_{A_1} + \omega_{E_2}$	$\frac{1}{d_5} = \varepsilon_{A_1'} + \omega_{E_1}$	$\frac{1}{d_6} = \varepsilon_{A_1'} + \omega_{E_2}$

finds

$$\begin{aligned}\phi^\dagger_{A_1} &= -\frac{2}{\sqrt{3}} c^\dagger_{B_1\uparrow} c^\dagger_{B_1\downarrow} + \frac{1}{\sqrt{3}}(c^\dagger_{E_x\uparrow} c^\dagger_{E_x\downarrow} + c^\dagger_{E_y\uparrow} c^\dagger_{E_y\downarrow}),\\ \phi^\dagger_{B_2} &= \frac{1}{\sqrt{2}}(c^\dagger_{E_x\uparrow} c^\dagger_{E_y\downarrow} + c^\dagger_{E_y\uparrow} c^\dagger_{E_x\downarrow}).\end{aligned} \tag{62}$$

These are readily verified for creating $W = 0$ pairs.

Appendix B. Pair binding energy

Here we calculate $\tilde{\Delta}$ for the B_2 pair in the CuO_4 cluster using second-order perturbation theory in both W and V and compare with Δ obtained by solving equations (37), (38). Basically the same holds for the A_1 pair. $\lambda_\eta \equiv 1$ throughout this appendix.

The ground state with two particles belongs to A_1 and, using the notation of table B.1, its energy reads

$$E(2) = 2\varepsilon_{A_1} + \frac{5}{16}U + U^2\left[\frac{3}{128\varepsilon_{A_1}} - \frac{61}{512}d_1\right] - g^2(d_2 + 2d_3) - g_{ox}^2(d_3 + d_4) + 2\sqrt{2}g_{ox}g d_3. \tag{63}$$

With three particles, the ground state is an E doublet, and

$$\begin{aligned}E(3) = 2\varepsilon_{A_1} + \frac{7}{16}U + U^2\left[\frac{5}{64\varepsilon_{A_1}} - \frac{53}{512}d_1\right] - g^2\left[d_2 + \frac{3d_3}{2} + \frac{d_5}{2}\right]\\ - g_{ox}^2\left[\frac{2}{\omega_{B_2}} + \frac{1}{2\omega_{E_1}} + \frac{1}{2\omega_{E_2}} + \frac{d_5}{4} + \frac{d_6}{4} + \frac{3d_3}{4} + \frac{3d_4}{4}\right] - g_{ox}g\left[-\frac{3\sqrt{2}d_3}{2} + \frac{\sqrt{2}d_5}{2}\right].\end{aligned} \tag{64}$$

The ground state with four particles belongs to B_2, as predicted by the canonical transformation; one gets:

$$\begin{aligned}E(4) = 2\varepsilon_{A_1} + \frac{9}{16}U + U^2\left[\frac{25}{128\varepsilon_{A_1}} - \frac{29}{512}d_1\right] - g^2[d_2 + d_3 + d_5]\\ - g_{ox}^2\left[\frac{8}{\omega_{B_2}} + \frac{1}{\omega_{E_1}} + \frac{1}{\omega_{E_2}} + \frac{d_3}{2} + \frac{d_4}{2} + \frac{d_5}{2} + \frac{d_6}{2}\right] + g_{ox}g\sqrt{2}[d_3 - d_2].\end{aligned} \tag{65}$$

Finally, using equation (1) and setting $\omega_\eta = \omega_0$, we obtain

$$\tilde{\Delta}(4) = -\frac{U^2}{16}\left[-\frac{1}{\varepsilon_{A_1}} - \frac{1}{2(-\varepsilon_{A_1} + \varepsilon_{A_1'})}\right] - g_{ox}^2\frac{4}{\omega_0}. \tag{66}$$

This must be compared with equation (38), section 5, that can be solved iteratively for $\Delta(4) = E - 2\varepsilon_{A_1}$ inserting $\varepsilon_{B_1} = 0$ from appendix A. The second iteration yields equation (66), supporting the identification $\tilde{\Delta}(4) = \Delta(4)$ at this order. Both quantities represent the effective interaction of the dressed B_2 $W = 0$ pair. Indeed, much information about the ground state energies cancels out if one applies equation (1); using the canonical transformation is a much more practical way to represent the effective interaction.

References

[1] For an overview, see Dagotto E 1994 *Rev. Mod. Phys.* **66** 763 and references therein
[2] Kohn W and Luttinger J M 1965 *Phys. Rev. Lett.* **15** 524
[3] Zanchi D and Schulz H J 1996 *Phys. Rev.* B **54** 9509
Zanchi D and Schulz H J 2000 *Phys. Rev.* B **63** 13609
Halboth C J and Metzner W 2000 *Phys. Rev. Lett.* **61** 7364
Honerkamp C and Salmhofer M 2001 *Phys. Rev. Lett.* **64** 184516
[4] Bickers N E, Scalapino D J and White S R 1989 *Phys. Rev. Lett.* **62** 961
Bickers N E and White S R 1991 *Phys. Rev.* B **43** 8044
Monthoux P, Balatsky A and Pines D 1991 *Phys. Rev. Lett.* **67** 3448
[5] Parola A, Sorella S, Parrinello M and Tosatti E 1991 *Phys. Rev.* B **43** 6190
[6] White S R, Chakravarty S, Gelfand M P and Kivelson S A 1992 *Phys. Rev.* B **45** 5062
[7] Hirsch J E, Tang S, Loh E and Scalapino D J 1988 *Phys. Rev. Lett.* **60** 1668
[8] Balseiro C A, Rojo A G, Gagliano E R and Alascio B 1988 *Phys. Rev.* B **38** 9315
[9] Cini M and Balzarotti A 1997 *Phys. Rev.* B **56** 14711
[10] Perfetto E, Stefanucci G and Cini M 2002 *Phys. Rev.* B **66** 165434
[11] Callegari A, Cini M, Perfetto E and Stefanucci G 2003 *Phys. Rev.* B **68** 153103
[12] Cini M, Balzarotti A, Brunetti R, Gimelli M and Stefanucci G 2000 *Int. J. Mod. Phys.* B **14** 2994
[13] Crowford M K, Kunchur M N, Farneth W E, McCarron E M and Poon S J 1990 *Phys. Rev.* B **41** 282
Crowford M K, Kunchur M N, Farneth W E, McCarron E M and Poon S J 1990 *Science* **250** 1390
Franck J P *et al* 1991 *Physica* C **185–189** 1379
Franck J P *et al* 1993 *Phys. Rev. Lett.* **71** 283
Franck J P 1994 *Physica* C **235–240** 1503
[14] McQueeney R J, Petrov Y, Egami T, Yethiraj M, Shirane G and Endoh Y 1999 *Phys. Rev. Lett.* **82** 628
[15] Shen Z X, Lanzara A, Ishihara S and Nagaosa N 2001 *Preprint* cond-mat/0108381
[16] Rösh O and Gunnarsson O 2003 *Preprint* cond-mat/0308035
[17] Ishihara S and Nagaosa N 2003 *Preprint* cond-mat/0311200
[18] Mazumdar S, Guo F, Guo D, Ung K C and Gammel J T 1996 *Proc. Discussion Mtg on Strongly Correlated Electron Systems in Chemistry (Bangalore, India)* (Berlin: Springer)
[19] Pao C H and Schuttler H B 1998 *Phys. Rev.* B **57** 5051
Pao C H and Schuttler H B 1999 *Phys. Rev.* B **60** 1283
[20] Lang I G and Firsov Y A 1963 *Sov. Phys.—JETP* **16** 1301
Lang I G and Firsov Y A 1964 *Sov. Phys.—Solid State* **5** 2049
[21] Wellein G, Roder H and Fehske H 1996 *Phys. Rev.* B **53** 9666
[22] Bonca J, Katrasnik T and Trugman S A 2000 *Phys. Rev. Lett.* **84** 3153
[23] Alexandrov A S and Ranninger J 1981 *Phys. Rev.* B **24** 1164
[24] Bar-Yam Y, Egami T, de Leon J M and Bishop A R 1992 *Lattice Effects in High-T_c Superconductors* (Singapore: World Scientific)
[25] Petrov Y and Egami T 2000 *APS, Annual March Meeting* vol Y20, p 3
[26] Cini M, Stefanucci G and Balzarotti A 1999 *Eur. Phys. J.* B **10** 293
[27] Cini M, Balzarotti A and Stefanucci G 2000 *Eur. Phys. J.* B **14** 269
[28] Cini M, Perfetto E and Stefanucci G 2001 *Eur. Phys. J.* B **20** 91
[29] Bersuker I B and Polinger V W 1989 *Vibronic Interactions in Molecules and Crystals* (Berlin: Springer)
[30] Grosso G and Parravicini G P 2000 *Solid State Physics* (San Diego, CA: Academic)
[31] Cini M and D'Andrea A 1988 *J. Phys. C: Solid State Phys.* **21** 193 and references therein
[32] Sakai T, Poilblanc D and Scalapino D J 1997 *Phys. Rev.* B **55** 8445
[33] Paturi P, Raittila J, Huhtinen H, Huhtala V-P and Laiho R 2003 *J. Phys.: Condens. Matter* B **15** 2103